Characterization of the Protrimer Intermediate in the Folding Pathway of the Interdigitated β-Helix Tailspike Protein†

Christopher B. Benton,‡,# Jonathan King,# and Patricia L. Clark*,§

Department of Biology, Massachusetts Institute of Technology, Cambridge, Massachusetts 02139, and Department of Chemistry & Biochemistry, 251 Nieuwland Science Hall, University of Notre Dame, Notre Dame, Indiana 46556

Received July 25, 2001; Revised Manuscript Received February 8, 2002

ABSTRACT: P22 tailspike is a homotrimeric, thermostable adhesin that recognizes the O-antigen lipopolysaccharide of *Salmonella typhimurium*. The 70 kDa subunits include long β-helix domains. After residue 540, the polypeptide chains change their path and wrap around one another, with extensive interchain contacts. Formation of this interdigitated domain intimately couples the chain folding and assembly mechanisms. The earliest detectable trimeric intermediate in the tailspike folding and assembly pathway is the protrimer, suspected to be a precursor of the native trimer structure. We have directly analyzed the kinetics of in vitro protrimer formation and disappearance for wild type and mutant tailspike proteins. The results confirm that the protrimer intermediate is an on-pathway intermediate for tailspike folding. Protrimer was originally resolved during tailspike folding because its migration through nondenaturing polyacrylamide gels was significantly retarded with respect to the migration of the native tailspike trimer. By comparing protein mobility versus acrylamide concentration, we find that the retarded mobility of the protrimer is due exclusively to a larger overall size than the native trimer, rather than an altered net surface charge. Experiments with mutant tailspike proteins indicate that the conformation difference between protrimer and native tailspike trimer is localized toward the C-termini of the tailspike polypeptide chains. These results suggest that the transformation of the protrimer to the native tailspike trimer represents the C-terminal interdigitation of the three polypeptide chains. This late step may confer the detergent-resistance, protease-resistance, and thermostability of the native trimer.

The average size of the proteins used for folding studies is considerably smaller than the average size of all known protein sequences (*1*). The longer chain length of larger proteins often results in chain diffusion processes and domain−domain interactions among distant sequence elements during folding. The native structures of many multimeric proteins possess structural features that result from the coupling of chain folding and chain assembly. Examples of such coupling include coiled-coils (*2*), collagen (*3*), multisubunit β-helices (*4*), and the triple-stranded β-spiral of the adenovirus tail fiber (*5*). Interdependent protein structure is also seen for extended polypeptide chain segments in multimeric proteins such as yeast RNA triphosphatases (*6*), and the protein subunits from RNP complexes, such as the large ribosomal subunit (*7*). The native structures of such proteins are uniquely dependent on interactions between residues on different subunit chains, and in many cases require extensive interdigitation, such as wrapping and/or clamping of the polypeptide chains around one another.

Studies by Baum and co-workers have demonstrated that proper "winding" of collagen strands requires an initial nucleation step (*8*). The nucleation step promotes proper polypeptide chain interdigitation and interchain contacts in the mature collagen sequences. Likewise, studies of smaller proteins that adopt quaternary structure, such as the dimeric arc repressor protein (*9*) and Trp repressor core domain (*10*), indicate that these polypeptide chains also acquire organized secondary or tertiary structure only upon interchain association. In fact, inspection of the arc repressor dimer crystal structure reveals interchain contacts over most of the amino acid sequence (*11*). In addition, there are numerous examples of multimeric proteins that acquire enzymatic activity only upon the formation of the final quaternary structure, such as bacterial luciferase (*12*). It should be noted that the rates of folding for large and/or multi-subunit proteins are often slow when compared to the rates of smaller, less complex proteins.

A large, multimeric protein with a folding pathway that involves the coupling of polypeptide chain folding and assembly is the *Salmonella typhimurium* phage P22 tailspike protein (Figure 1). Tailspike is one of the very few proteins whose in vivo folding intermediates as well as in vitro folding intermediates have been identified. The mature protein is a homotrimer of 666 amino acid residue polypeptide chains. The native structure is SDS- and protease-resistant, and unfolds only under environmentally harsh conditions, such as high temperature (>80 °C), or the presence of 5 M urea and acidic (pH 3) conditions (*13, 14*). The resistance of the

† This work was supported by the National Institutes of Health (GM17980 to J.K.). P.L.C. was supported by a postdoctoral fellowship from the NIH (GM19715) at MIT and by an award from the Clare Boothe Luce Program at the University of Notre Dame.

* To whom correspondence should be addressed: Phone: (574) 631−8353; fax: (574) 631−6652; e-mail: pclark1@nd.edu.

Massachusetts Institute of Technology.

§ University of Notre Dame.

‡ Present address: Baylor College of Medicine, One Baylor Plaza, Box 14, Houston, TX 77030

10.1021/bi0115582 CCC: $22.00
Published on Web 03/29/2002

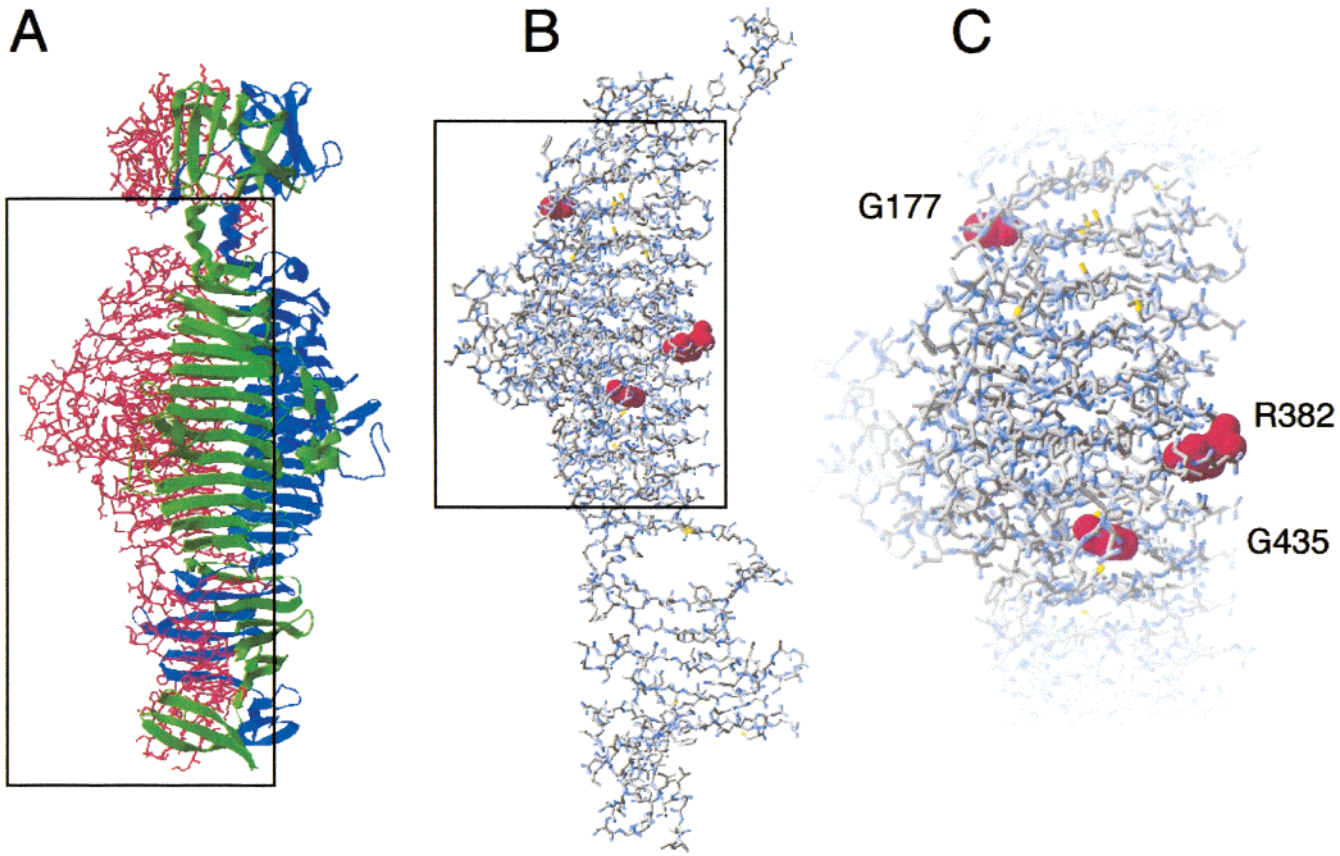

FIGURE 1: Crystal structure of P22 tailspike (*15*). (A) Native trimer structure, solved by X-ray crystallography (*15*), showing the N-terminal domain (top; crystallized separately), central β-helix domains, and C-terminal interdigitation and β-sheet domains (bottom). Two subunits are depicted as ribbon diagrams (green and blue polypeptide chains); the third subunit is depicted as a line diagram (red polypeptide chain). (B) Structure of one tailspike polypeptide chain from the native trimer crystal structure (boxed area in panel A). The N-terminal domain has been omitted for clarity. The sites of *tsf* mutations used in this study (G177, R382, and G435) are shown as red space-filling models. (C) Enlargement of the tailspike β-helix domain (boxed area in panel B). G177 is largely exposed in the native structure. R382 is completely buried due to interactions with the other two tailspike subunits (not shown; see panel A). R382 also participates in an "arginine stack" involving arginine side chains from successive rungs of the β-helix. G435 is largely, although not entirely, buried from solvent.

native trimer to denaturation and digestion presumably reflects its function as an external structural protein of the P22 virion, responsible for host recognition and infection. The native structure of each monomer chain is dominated by a central 13-rung parallel β-helix domain (*15*), where the β-helices dock against one another along the long axis of the helix (Figure 1A). At the C-termini of the β-helices, the three polypeptide chains wrap around one another to form an interdigitated parallel β-prism domain (*4*). This feature appears to function as a molecular clamp, contributing to the stability of the trimeric native state. From the crystal structure (*15*, *16*), it is apparent that during the folding of tailspike, the three chains must interdigitate at the C-terminus to form the parallel β-prism; thus, tailspike folding and subunit assembly are concomitant processes. However, it is not clear from the crystal structure how or when the interdigitation of the three monomer chains occurs during folding, or what mechanism promotes correct (and avoids incorrect) interdigitation.

For β-sheet domains in general, very little is known about the conformation of β-strand sequences prior to their assembly into β-sheets. Folding experiments with small β-sheet proteins indicate β-sheet domains may first form an intermediate with substantial sheet topology, but lacking a stable hydrogen bond network (*17*, *18*). Within the cell, newly synthesized tailspike polypeptide chains may carry out the initial steps of β-helix folding while still associated with the ribosome (*19*). However, during in vitro refolding, the early conformation of sequences that will eventually be incorporated into β-sheets, but do not form early during folding—such as those requiring prior assembly of other structural elements—remains unclear.

Tailspike folding occurs on the order of minutes in vivo, or on the order of hours at lower temperatures in vitro (*20*, *21*). The chains populate monomeric, dimeric, and trimeric intermediates before production of the native tailspike structure (as illustrated in Figure 2A). The trimeric intermediate is referred to as protrimer (Pt),[1] and this species is believed to be a precursor to the native trimer (Nt) (*14*, *20*). The protrimer is transient, much less stable than native tailspike, and SDS-sensitive. The relative instability of the protrimer species suggests its individual β-helix domains may have associated, but the C-termini have not yet interdigitated to confer the native state stability. The monomeric, dimeric, and protrimer intermediates of productively folding tailspike can be trapped at cold temperatures, and resolved using nondenaturing gel electrophoresis (*22*). On a nondenaturing

[1] Abbreviations: [M], monomeric tailspike folding intermediates; [D], dimeric tailspike folding intermediates; Pt, tailspike protrimer intermediate; Nt, tailspike native trimer; EDTA, disodium ethylenediamine tetraacetate; GSH, reduced glutathione; GSSG, oxidized glutathione; *tsf*, temperature-sensitive folding.

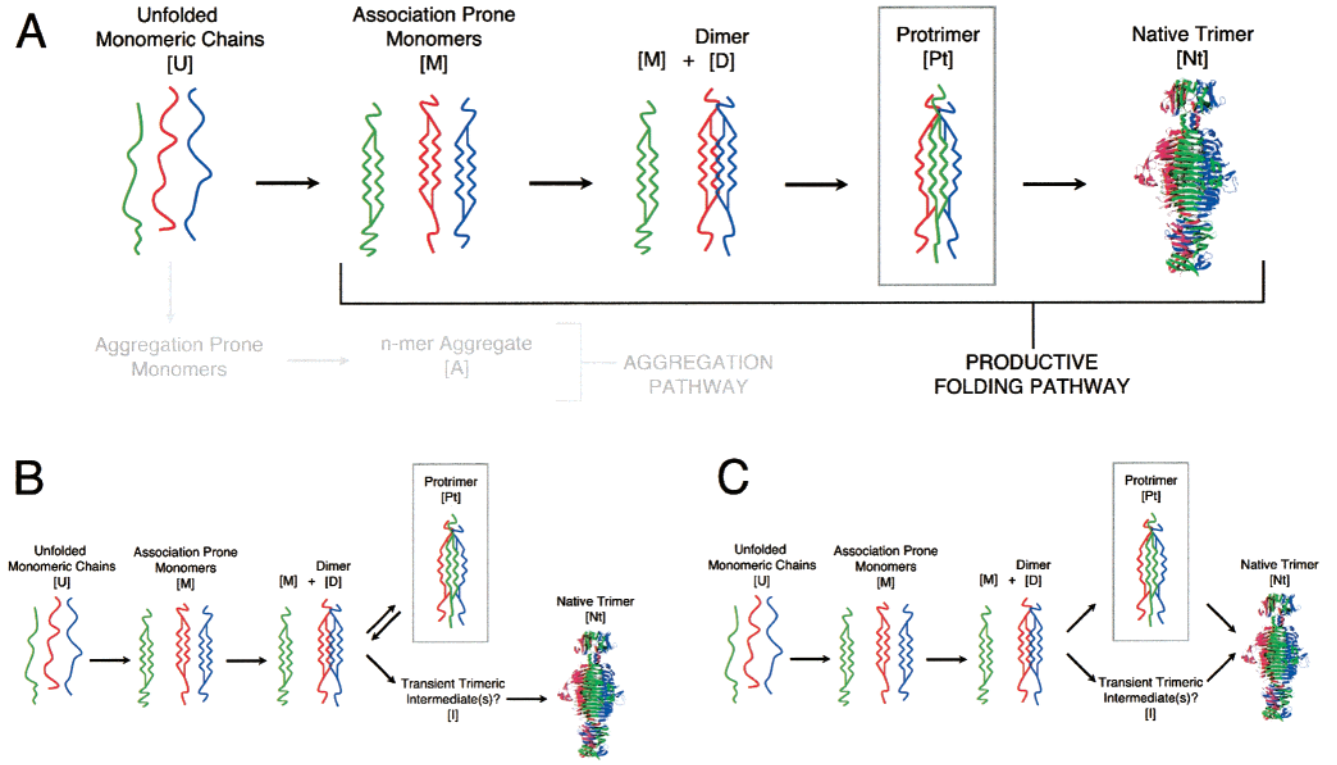

FIGURE 2: Putative productive folding pathways for P22 tailspike. (A) Predicted pathway for productive folding, suggested by previous studies (*14*, *22*). Two folding-competent monomers ([M]) dock to become a dimer ([D]). Dimer and monomer dock to form the protrimer (Pt) intermediate. The protrimer (boxed in figure), the focus of this work, migrates as a distinct band, separate from native trimeric tailspike (Nt) conformations on a nondenaturing polyacrylamide gel (see Figure 3A). Protrimer folds further to native trimeric tailspike, making it an obligate trimeric intermediate on the productive folding pathway. (B) Alternative folding pathway: off-pathway protrimer. In this mechanism, protrimer represents an off-pathway folding trap, and reversibly unfolds to a monomer and dimer, which can reassociate into native tailspike, potentially via an unknown transient folding intermediate. (C) Alternative folding pathway: parallel folding pathways. In this alternative pathway, protrimer is one, but not the only, trimeric intermediate on the productive folding pathway to native tailspike.

gel, protrimer migrates more slowly than native trimer, while the monomeric and dimeric intermediates migrate more quickly (Figure 3A) (*20*, *22*, *23*). Protrimer migrates as a well-resolved band (*20*), indicating a long-lived intermediate consisting of a small conformational ensemble. The protrimer intermediate forms well in advance of the SDS-resistant native trimer (compare Figure 3, panels A and B).

Studies by Seckler and co-workers have shown that the native state fluorescence and circular dichroism spectra appear early in the folding of the tailspike polypeptide chain, prior to chain association (*14*, *21*, *24*), and are therefore unsuitable probes for studying the conversion of protrimer to native trimer. The overall rate of tailspike folding is independent of protein concentration (*21*), indicating that the Pt → Nt conformational transition may represent the rate-limiting step for the tailspike folding mechanism.

Each tailspike polypeptide chain contains eight cysteine residues, all of which are buried and reduced in the native structure (*15*). However, the protrimer intermediate contains interchain disulfide bonds (*25*). These disulfide bonds are reduced during the conversion from protrimer to native trimer. Tailspike proteins incorporating single Cys → Ser substitutions exhibit defects in chain folding and/or assembly kinetics. However, once the mutant proteins are folded, the single Cys → Ser substitutions do not affect to the stability or activity of the native state (*26*). A subset of cysteine residues near the C-terminus appears important for efficient folding and assembly. Tailspike polypeptide chains incorporating mutations of two Cys residues near the C-terminus are unable to form the native trimer structure (*26*). It is possible that the disulfide bonds of the protrimer align and/or stabilize this precursor conformation, prior to the interdigitation step. The electron donor/acceptors for the presumed redox reaction have not been identified, but the tailspike sequence also contains a thioredoxin-like C−X−X−C sequence motif, suggesting a possible internally catalyzed oxidation/reduction reaction.

The protrimer to native trimer transition represents an unusually large shift in native gel mobility for two species of the same molecular weight (see Figure 4). Presumably, this shift arises from a significant alteration of molecular shape and/or net surface charge during the Pt → Nt transition, as these two characteristics define the mobility of a protein through nondenaturing gels (*27*, *28*). To resolve this question, we have examined the mobilities of the native tailspike trimer and the protrimer intermediate to characterize properties of the protrimer, and the nature of the Pt → Nt conversion. The conformational change that occurs during the isomerization of protrimer to native trimer may reflect the interdigitation of the C-termini of the three polypeptide chains.

EXPERIMENTAL PROCEDURES

Purification of Tailspike Proteins. Wild-type tailspike and tailspike *tsf* mutant proteins (*13*, *29*) were produced from P22 infection of *S. typhimurium* strain DB7136 (*30*). Protein was produced and purified as described previously (*31*). Briefly, 1 L of Super Broth (32 g/L tryptone, 20 g/L yeast

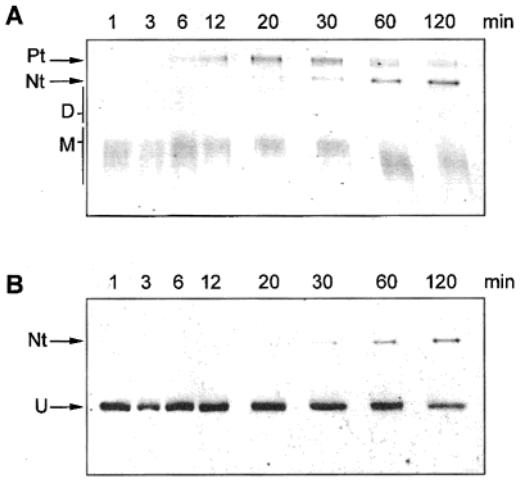

FIGURE 3: Migration of tailspike refolding intermediates on native and denaturing polyacrylamide gels. (A) Native gel migration of tailspike refolding intermediates. Monomeric (M) and dimeric (D) intermediates are visible as wide smears near the bottom of the gel. The mobility of the protrimer (Pt) species is distinctly retarded with respect to the mobility of the native trimer (Nt), despite the same molecular composition. Unlike the monomeric and dimeric intermediates, protrimer migrates as a well-resolved band. (B) SDS gel migration of tailspike refolding intermediates. As only the native trimer is resistant to SDS denaturation, the migration of all other intermediates converts to that of SDS-denatured tailspike chains (U). Note that the native SDS-resistant trimer appears at the same time or slightly later than the appearance of the native gel species with native trimer mobility, demonstrating that SDS-resistance occurs only upon conversion of the protrimer species to the native trimer structure.

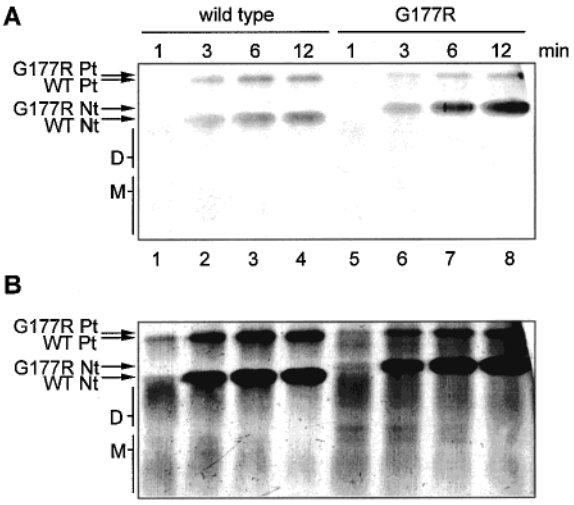

FIGURE 4: Migration of wild type and mutant tailspike refolding intermediates on an 8% nondenaturing polyacrylamide gel. (A) Left lanes: refolding of wild-type tailspike; right lanes: refolding of *tsf* mutant G177R tailspike chains. Note that the relative mobilities of the wild type and G177R native trimers are different, as are the mobilities of the two protrimer species. (B) For illustrative purposes, the gel shown in panel A is shown here at a lower contrast threshold to highlight the monomeric and dimeric tailspike intermediate ensembles.

extract, 5 g/L NaCl, pH to 7.5) was innoculated with 10 mL of an overnight culture of DB7136. Cells were grown at 30 °C to ~4 × 10^8 cells/mL and infected (moi = 10) with bacteriophage P22 *5⁻amN114/13⁻amH101* (amber mutations in the capsid and lysis genes prevent capsid assembly and delay cell lysis, respectively) (*32*). Three hours after phage infection, cells were harvested by centrifugation at 3000*g* for 5 min. Cells were resuspended in buffer B (50 mM Tris, pH 7.6, 25 mM NaCl, 2 mM EDTA) with 40 mM octoglucoside. Cells were lysed with two freeze/thaw cycles, and cell debris was removed by centrifugation at 12000*g* for 20 min. The supernatant was further clarified by ultracentrifugation at 159000*g* for 1 h, and saturated with 40% ammonium sulfate to precipitate and partially purify tailspike. The resulting precipitate was resuspended in buffer B and dialyzed against buffer B overnight. Tailspike was further purified using FPLC ion exchange chromatography with a DEAE resin (Sepharose Fast Flow, Amersham Pharmacia Biotech), using 50 mM Tris, pH 7.6, with 2 mM EDTA, and a 0 to 100 mM NaCl gradient. Purified tailspike was dialyzed against buffer B. Finally, the sample was subjected to hydrophobic chromatography with a hydroxyapatite column (Bio-Rad) equilibrated in buffer B. Tailspike eluted in the column void volume and appeared as single band on Coomassie and silver stained gels (data not shown).

Tailspike Refolding. Tailspike was refolded using a previously described protocol (*22*). Native P22 tailspike (2 mM) was denatured in 6 M urea, 50 mM phosphate, pH 3. Refolding was initiated by rapid 20-fold dilution with ice-cold refolding buffer (40 mM phosphate, 1 mM EDTA, pH 7.6). The refolding mixture was incubated in an ice−water bath. After 20 min at 0 °C, the reaction mixture was shifted to a refrigerated 20 °C water bath. To follow the production of structured intermediates and native tailspike trimer, aliquots were removed at various time points and rapidly transferred to tubes containing ice-cold 3× nondenaturing sample buffer (15 mM Tris, 120 mM glycine, 30% glycerol, bromophenol blue), or 3× SDS sample buffer [19 mM Tris pH 6.8, 2% SDS final (2%), 15 mM DTT, 30% glycerol, bromophenol blue].

For refolding experiments with controlled redox potentials, the pH of the refolding buffer was adjusted to 8.3. In these experiments, reduced and oxidized glutathione were mixed in various ratios, such that the total final concentration ([GSH] + [GSSG]) was 5 mM.

Electrophoresis and Staining. Nondenaturing and SDS polyacrylamide gel electrophoresis was performed at 4 °C as described previously (*33*). Unless otherwise stated, resolving and stacking gels were made with 9 and 4.3% acrylamide, respectively. In general, gels were made to a thickness of 1.5 mm, and run for 5−6 h at a constant current of 15 mA. For Ferguson plot analysis, special care was taken to make gels precisely level, no stacking gel was used, and gels were run for exactly 5 h. Silver staining was carried out as previously described (*34*), with the exception that the gels were treated with 2.5 mM sodium thiosulfate for 6 min instead of 2 min.

Kinetic and Ferguson Plot Analysis. The fraction of total polypeptide chains in each intermediate state during each refolding time point was determined by quantification of silver stained gel bands with a Molecular Dynamics Personal densitometer and ImageQuant software (Molecular Dynamics). The intensity of the silver staining was linear within the protein concentration range examined (data not shown). Kinetic simulation, analysis, and fitting were performed using the program DynaFit (BioKin) (*35*). Nonlinear least-squares regression of the experimental data (*36*) was performed using the Levenberg−Marquardt algorithm (*37*). Ferguson plots were constructed using gel mobility measurements for

Table 1: Rate Constants and Global Fitting Results for Tailspike Refolding Mechanisms

mechanism	scheme	rate	value	fit result
simple sequential	M + M → D	k1	2300 ± 200 M^{-1} s^{-1}	converge
(Figure 2A)	M + D → Pt	k2	13000 ± 2000 M^{-1} s^{-1}	
	Pt → Nt	k3	0.008 ± 0.003 s^{-1}	
off-pathway protrimer	M + M → D	k1	2400 ± 200 M^{-1} s^{-1}	nonconverge
(Figure 2B)	M + D → Pt	k2	2.1 × 10^7 ± 7 × 10^9 M^{-1} s^{-1}	
	Pt → M + D	k-2	13 ± 4400 s^{-1}	
	M + D → Nt	k3	15000 ± 3000 M^{-1} s^{-1}	
non-obligate protrimer	M + M → D	k1	2300 ± 300 M^{-1} s^{-1}	nonconverge
(Figure 2C)	M + D → Pt	k2	8000 ± 10000 M^{-1} s^{-1}	
	M + D → Nt	k3	0.004 ± 0.006 M^{-1} s^{-1}	
	Pt → Nt	k4	5000 ± 10000 s^{-1}	

protrimer and native trimer bands on 6.5, 7.0, 7.5, and 8.0% polyacrylamide gels (*38*). The relative molecular radii of tailspike species were determined in part using the program ElphoFit (*39*).

RESULTS

Resolution and Kinetic Behavior of the Tailspike Protrimer in Vitro. To confirm that the protrimer is an on-pathway precursor to native tailspike trimer, we investigated the appearance and disappearance of tailspike folding intermediates during refolding in vitro. Intermediates of the tailspike refolding pathway were resolved using nondenaturing gel electrophoresis (*22*, *33*). Tailspike was denatured in acid-urea buffer (*14*), and incubated at 0 °C on wet ice. Refolding reactions were initiated by 20-fold dilution with refolding buffer at 0 °C, incubated for 20 min, and then shifted to 20 °C for the remainder of the refolding reaction. The 0 °C incubation step inhibits off-pathway aggregation in vitro such that ~80% of tailspike polypeptide chains refold to native trimer under these conditions (*22*). Refolding at 0 °C permitted the polypeptide chains to adopt the structured monomer conformation; however, no later refolding and/or assembly intermediates were formed: the distribution of refolding intermediates remained unchanged as detected by native gel electrophoresis (*22*, and data not shown). The accumulation of productive structured monomer conformations results in an increase in the overall refolding rate when the temperature is raised to 20 °C, versus refolding without the cold incubation step (*21*, *22*). At various refolding times, aliquots were diluted into ice-cold buffer to trap the later refolding intermediates. The polypeptide chains in these samples were separated using nondenaturing gel electrophoresis in the cold (*20*).

Gel bands corresponding to native tailspike and tailspike refolding intermediates were visualized by silver staining (Figures 3 and 4), and the relative amounts of tailspike polypeptide chains in the native state and each intermediate population were determined by laser densitometry. Plots of these quantities versus time (Figure 5) show the steady disappearance of structured monomeric species, the slower disappearance of dimeric intermediates, the appearance and slow disappearance of protrimer, and the steady accumulation of native tailspike trimer. This technique only partially resolved the conversion of monomeric tailspike chains into dimeric intermediates; this limitation introduced additional error into the kinetic fitting (see below).

Results were fit to potential tailspike folding mechanisms using iterative refinement of kinetic simulations via global

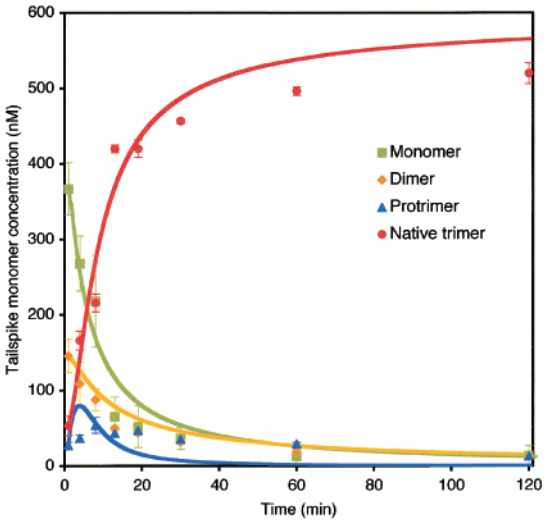

FIGURE 5: Tailspike refolding kinetics as determined by nondenaturing gel electrophoresis. Data points represent the quantification of gel bands corresponding to monomeric (green), dimeric (orange), protrimer (blue), and trimer (red) tailspike species during refolding in vitro (average of three experiments). Data points collected during the initial ice incubation step (t = −20−0 min) showed no detectable change in the concentration of [M] or [D] and are not included in the figure. Error bars represent the standard deviation from three separate experiments. Lines correspond to the best fit of the experimental data to the simple sequential folding pathway illustrated in Figure 2A; relevant kinetic parameters are listed in Table 1.

analysis. We began with a simple sequential model for native trimer production (Figure 2A and Table 1), where protrimer is an obligate, productive precursor to the native trimer structure. This model includes a second-order rate constant for the conversion of monomeric and dimeric intermediates to the protrimeric intermediate. Previous experiments have indicated that the rate of subunit association (measured as the loss of the ability to form heterotrimers during refolding) is concentration independent, perhaps via an undetected rate-limiting monomeric rearrangement (*21*). However, native gel electrophoresis allows measurement only of the production of the protrimeric species, and does not permit direct measurement of the kinetics of subunit exchange. As a result, the data shown here was fit to the simplest possible model, but it is quite possible that the deviation seen between the experimental populations of protrimer and the calculated fit (Figure 5) is a result of one or more unobservable intermediate steps in the refolding mechanism.

Refolding results were also fit to two other simulated folding mechanisms: one with protrimer representing an off-pathway, unproductive intermediate (Figure 2B and Table

1), and the other with protrimer as a productive, but nonobligate intermediate (parallel pathway; Figure 2C and Table 1). These pathways represent viable alternative refolding mechanisms because they both are qualitatively consistent with the observation that the protrimer intermediate first accumulates and then dissipates on a denaturing gel (Figure 5) (*20*). The refolding results (Figure 5) fit most closely to the simple sequential model for tailspike folding (Figure 2A), resulting in rates of 2300 M^{-1} s^{-1}, 13000 M^{-1} s^{-1}, and 0.0076 s^{-1}, respectively, for the three forward reactions listed in Table 1. The limitations of the electrophoretic separation and staining assay, as well as potential unobserved kinetic steps, resulted in significant error in these measurements (Figure 5; Table 1). However, global fitting to the two alternative folding mechanisms resulted in unacceptably poor fits.

The Effect of Glutathione on Protrimer Production and Evolution in Vitro. Previous results have shown that protrimer contains transient interchain disulfide bonds (*25*, *34*). We investigated whether addition of oxidized glutathione, the primary oxidizing agent in vivo, would trap refolding tailspike chains at the protrimer intermediate in vitro, increasing the concentration of this intermediate in the refolding reaction. Reduced (GSH) and oxidized glutathione (GSSG) were added to tailspike refolding reactions in varying ratios, and samples from various refolding time points were analyzed by nondenaturing gel electrophoresis. Under completely reducing conditions (5 mM GSH, 0 mM GSSG), tailspike refolded to native trimer with high yield, but the protrimer was not well populated (data not shown). However, under entirely oxidizing conditions (5 mM GSSG, 0 mM GSH), no native trimer was detected, nor was a band for protrimer detected (data not shown). This confirms similar results obtained by Frank Furst and Robert Seckler at Potsdam (personal communication). For intermediate ratios of GSH:GSSG, increased native tailspike production was observed as the refolding environment became more reducing. Thus, in these experiments, addition of redox agents did not increase the intensity or definition of the protrimer band as compared to the band observed for tailspike refolding in the absence of controlled redox conditions.

Protrimer and Native Trimer Tailspike Have the Same Surface Charge Densities But Different Molecular Radii. As mentioned above, the tailspike protrimer and native trimer have significantly different mobilities in nondenaturing polyacrylamide gels (Figures 3 and 4). To explore this further, we examined the mobilities of protrimer and native trimer as a function of acrylamide concentration. Extrapolation of gel mobility to 0% acrylamide provides information on the net surface charge of a macromolecule. The slope of the mobility as a function of acrylamide concentration yields information on the molecular radius of the macromolecule (*38*). Theoretical plots of the log of the gel retention factor versus acrylamide concentration are shown in Figure 6A, with a description of the analysis of these plots (*27*).

Tailspike was refolded as described above. Refolding samples were chosen from four early time points to detect the protrimer and earlier refolding intermediates. These samples were electrophoresed in the cold on nondenaturing polyacrylamide gels of varying acrylamide concentrations. Special care was taken to make the gels precisely level, and gels were run for exactly 5 h. To reduce variation between individual gels, the stacking gel was omitted. The migration of bands corresponding to tailspike protrimer and native trimer bands was measured.

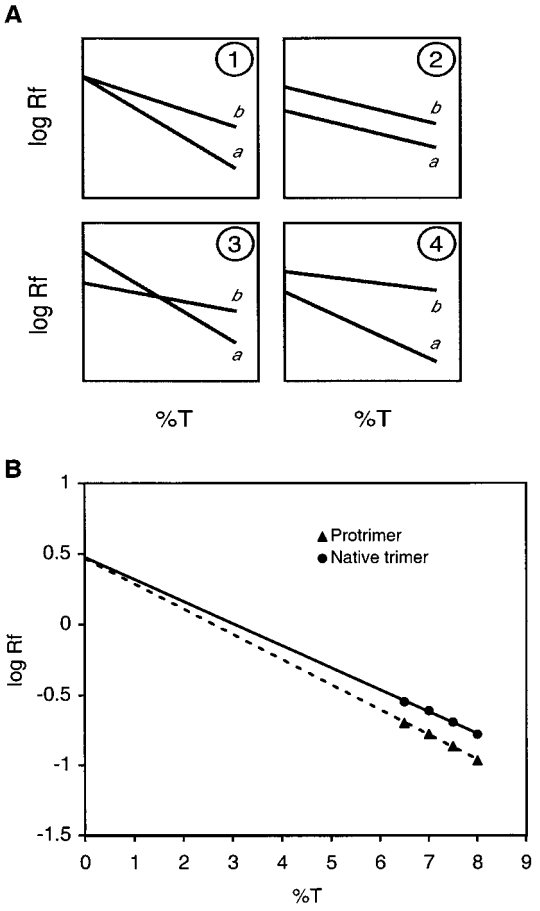

FIGURE 6: Ferguson plot analysis of tailspike native trimer and protrimer intermediate. (A) Theoretical Ferguson plots, adapted from Hames (*27*), describing four alternative relationships between two molecular species. Each plot depicts the log of the retention factor (log R_f) as a function of acrylamide concentration (%*T*). Situation 1: Two proteins, a and b, have the same net surface charge, and their difference in migration is due entirely to difference in their respective molecular radii; a is larger than b. The Ferguson plots have identical Y-intercepts, indicating that the two proteins would have the same mobility if subjected to electrophoresis in free solution (free mobility). Situation 2: Proteins a and b have the same molecular radius, and differ only in net surface charge; b has a more negative net charge. As a result, varying the gel concentration has no effect on their relative gel mobilities. Situation 3: Protein a has a larger molecular radius (more negative slope), and also a more negative net charge (has the larger free mobility; moves more quickly in free solution). In this case, separation based on size is antagonistic to separation based on charge. Situation 4: Protein a has a larger molecular radius and a more positive net charge; protein b is smaller and has a more negative net charge. Size and charge are therefore synergistic in their effects on separation of the two proteins. (B) Data points represent gel migration behavior (retention factor (R_f)) of native trimer (circles) and protrimer (triangles) in nondenaturing gels of increasing density. Lines correspond to the best linear fit through the data; for native trimer (solid line) $R^2 = 0.994$, for protrimer (dashed line), $R^2 = 0.997$. Slopes and Y-intercepts are listed in Table 3.

The log of the retention factors of the native trimer and protrimer was plotted versus the percentage of acrylamide. Gels with acrylamide percentages below 6% were not experimentally feasible, as the resulting gels were too fragile to manipulate. Nevertheless, the data corresponded very well to a linear fit ($R^2 > 0.99$) supporting the validity of the extrapolation to 0% acrylamide (Figure 6B). The linear fits

Table 2: Tailspike *tsf* Mutation Locations and Charge Changes.

mutation		location of amino acid	charge change for monomer	charge change for trimer
G177R	glycine → arginine	exterior; exposed edge of second rung	+1	+3
R382S	arginine → serine	interior of eighth rung; part of arginine stack	−1	−3
G435R	glycine → arginine	mostly buried; turn of ninth rung	+1	+3

for protrimer and native trimer yielded similar Y-intercepts, but different slopes. Thus, protrimer and native tailspike would exhibit similar migration through an electric field in free solution, and are therefore likely to possess similar net surface charge. This suggests that their separation in a nondenaturing gel is due to protrimer having a larger molecular radius, and thus migrating more slowly than native tailspike; similar behavior has been previously observed for the elution of protrimer and native protrimer from size exclusion columns (*14*). If tailspike were a globular protein, and it and its intermediates could therefore be accurately represented by spheres, the Pt → Nt transition would represent a ~10% reduction in molecular radius (*39*). However, the crystal structure of tailspike shows that its actual molecular shape is significantly different from spherical (Figure 1A). As a result, a theoretical calculation of size change based on spherical volumes is likely to be of limited value.

Effects of Charge-Change Mutations on the Gel Mobility of Protrimer and the Native Trimer. Temperature sensitive folding (*tsf*) mutations prevent chain folding and assembly at high (restrictive, >37 °C) temperatures, but not at lower (permissive, <30 °C) temperatures (*23*, *29*). A subset of tailspike *tsf* mutations has amino acid substitutions with altered charge with respect to wild-type tailspike (*40*). These amino acid substitutions alter the gel mobility of the native state of the mutant tailspike trimer (Figure 4). We investigated three mutant proteins (G177R, R382S, and G435R) that alter the overall charge of the protein (Table 2), and are located at distinct positions along the length of the β-helix domain (Figure 1C) as probes of protrimer surface charge and conformation. At permissive temperatures, all three mutant proteins refold to the native tailspike structure, and the thermal stability and activity of the native mutant proteins are indistinguishable from the wild-type trimer (*29*, *41*). Residue G177 is very exposed, residue R382 is buried within the body of the tailspike protein, and residue G435 is partially exposed (Figure 1C). G177R and G435R mutations change a neutral residue to a positive residue, resulting in an overall charge change of +3 for the homotrimeric tailspike. The R382S mutation changes a positive residue to a neutral residue, with an overall charge change of −3 for the trimer (Table 2). To reveal structural differences between the protrimer and native trimer structures, we examined the effects of the three mutations on the mobilities of the native tailspike trimer and protrimer species, using nondenaturing gel electrophoresis. Ferguson plots comparing native trimer mobility to protrimer mobility are shown for each of the three mutant proteins in Figure 7.

The Ferguson plot for the G177R mutant tailspike reveals that, similar to wild type tailspike, the mutant native trimer and protrimer species have similar surface charge densities

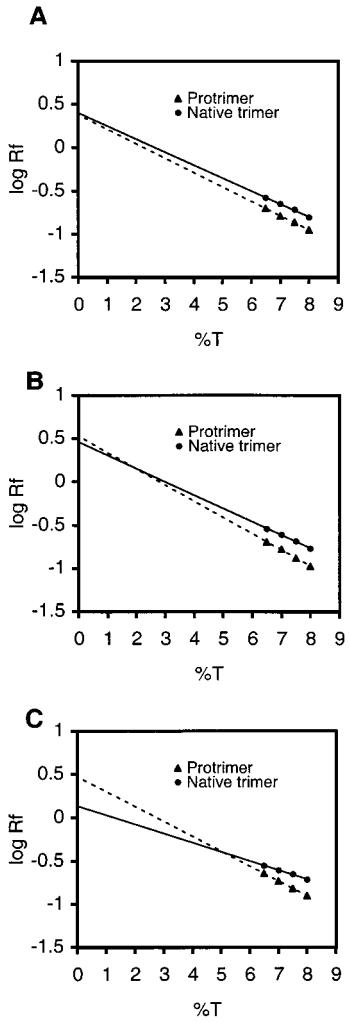

FIGURE 7: Ferguson plots for mutant tailspike native trimers and protrimers. Plots are shown for (A) G177R, (B) R382S, and (C) G435R. Data are presented as in Figure 6; slopes and Y-intercepts are listed in Table 3.

(Figure 7A). However, the net surface charge for these species was different than that observed for wild type native trimer and protrimer (Table 3). This is expected for a charge change substitution that affects equally the surface charge of both protrimer and native trimer. Consistent with this, the tailspike crystal structure suggests that the replacement arginine side chain will be exposed on the surface of the native trimer (Figure 1C). The slopes of the Ferguson plots reveal that both of these species have slightly different molecular radii than wild type (Figure 7A, Table 3), potentially due to the effect of the mutation.

The Ferguson plot for the R382S mutant tailspike establishes that this mutant native trimer species has structural characteristics very similar to that of the wild-type native trimer, for both molecular radius and net surface charge (Figure 7B, Table 3). This result suggests the R382S charge change is not exposed on the surface of the native trimer, consistent with the position of R382 in the tailspike crystal structure (Figure 1C). The R382S protrimer, however, behaves unlike the wild-type protrimer: net surface charge and molecular radius are both affected (Figure 7B, Table 3). This result suggests that the mutated side chain is exposed in the protrimer conformation, or affects other residues that in turn alter the surface charge.

Table 3: Ferguson Results for Wild Type and *tsf* Mutant Tailspike Proteins[a]

		Ferguson plot results		comparison to wild-type tailspike	
tailspike	refolding species	Y-intercept	slope	net surface charge	molecular radius
wild type	protrimer	0.467	−0.41		
	native trimer	0.476	−0.36		
G177R	protrimer	0.380	−0.38	more positive	smaller
	native trimer	0.401	−0.35	more positive	no significant change
R382S	protrimer	0.524	−0.43	more negative	larger
	native trimer	0.458	−0.35	slightly more positive	no significant change
G435R	protrimer	0.470	−0.40	no significant change	no significant change
	native trimer	0.134	−0.24	much more positive	much smaller

[a] Results are the mean of at least three experiments with standard deviation not exceeding 4%.

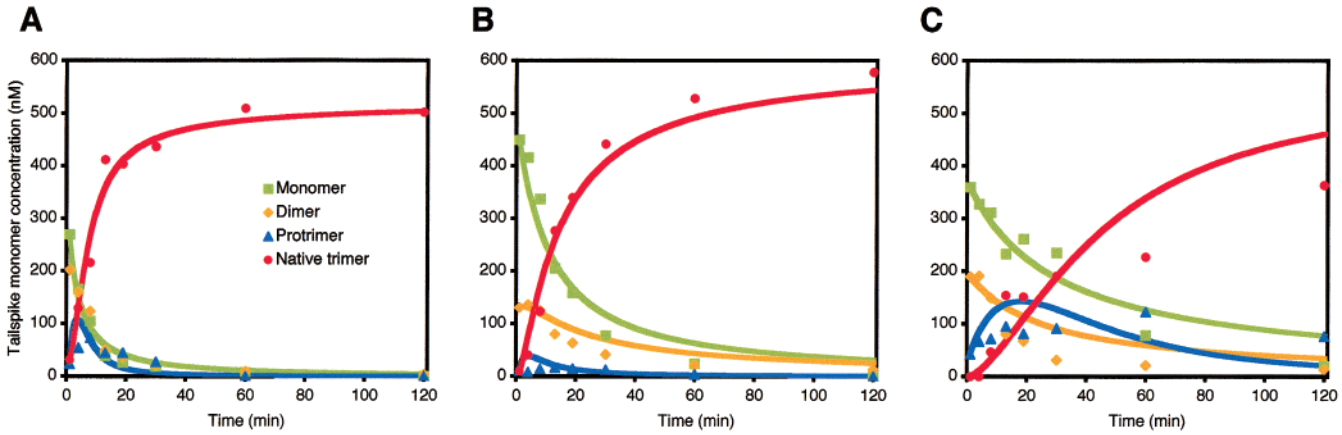

FIGURE 8: Refolding kinetics for mutant tailspike proteins. Plots are shown for (A) G177R, (B) R382S, and (C) G435R. Data are presented as in Figure 5. The amount of error is very similar to the results shown in Figure 5; error bars have been omitted for clarity.

The native G435R trimer produced a Ferguson plot that was dramatically different from that of wild type native trimer (Figure 7C). This change represented a severe alteration of both surface charge and molecular radius for the native G435R tailspike, consistent with a radical substitution at a partially surface-exposed position (Figure 1C). Conversely, the Ferguson plot for the G435R protrimer is very similar to the plot for wild type protrimer. This suggests that the G435R mutation is not exposed on the surface of the protrimer conformation. One possibility is that the C-terminal regions of each polypeptide chain are folded back onto the β-helix domains, effectively shielding the G435R region of the β-helix in the protrimer conformation.

Kinetics of Protrimer and Native Trimer Formation for Mutants. Since the mutant tailspikes described here represent temperature-sensitive folding mutations, they fail to reach the native state at high temperature, but do fold correctly at permissive temperatures (*23*, *29*, *41*). At restrictive temperatures, the folding defect is due to the thermal instability of the mutant monomer intermediate, and the protrimer intermediate is not formed (*23*). However, at permissive temperatures it is possible to detect defects with chain association in the protrimer to native trimer conversion. We examined the kinetics of refolding at a permissive temperature (20 °C) for each of the three charge-change mutants, and compared the refolding to that of wild-type tailspike.

Refolding of the G177R tailspike mutant occurred with rates that were very similar to wild type tailspike refolding (Figure 8A). The R382S protein chains also showed excellent refolding under these conditions (Figure 8B). In fact, this mutant refolded with a slightly higher yield of native tailspike. In addition, there was very little protrimer intermediate detected during refolding. The distributions of tailspike refolding species throughout R382S refolding were comparable to those of wild-type refolding experiments in the presence of 5 mM GSH, where the refolding yield was high and a very small amount of protrimer accumulated.

G435R had productive refolding kinetics most unlike wild type at this permissive temperature (Figure 8C). The rate and yield of tailspike trimer production was significantly depressed during the time course of the experiment. The protrimer population accumulated, but disappeared only very slowly over the course of the refolding experiment. While productive folding was observed, it was coexistent with extensive formation of larger tailspike aggregates (not shown).

DISCUSSION

The results reported here corroborate that protrimer is an on-pathway, productive intermediate formed during refolding in vitro, as indicated by the results of Seckler and co-workers (*14*). The formation of the mature tailspike trimer represents the formation of a C-terminal β-sheet structure with strands donated by each of the three subunits (Figure 1A). These strands cannot be partnered with each other in their monomeric state. To date, no examples exist of an isolated, structured β-strand or isolated β-sheet domain [i.e., free from the packing of other structural elements, such as another β-sheet (*42*) or an α-helix (*43*)]. The conformation and organization of the sequences that participate in multimeric β-sheets, including the β-prism of the native tailspike trimer, must therefore be arranged in some non-native conformation in earlier intermediates. The results presented here indicate

that the transition from these non-native conformations to the interdigitated sheet occurs in the Pt → Nt conversion. Recent studies of mutants in this region indicate that the interdigitated region acts as a molecular clamp to achieve the high stability of the native trimer (*44*). For collagen, the complex multi-subunit structural unit seen in the native state is achieved through the use of C-terminal registration domains which bring the polypeptide chains together in proper register before the formation of the native triple-helix (*3*). These registration domains are stabilized by interchain disulfide bonds (*45*).

Structural Comparison of the Protrimer Intermediate to Native Trimer. The Ferguson plots of wild type native trimer and protrimer reveal that these two conformations have similar net surface charge, while they differ markedly in molecular radius; the difference in molecular radius was previously detected by size-exclusion HPLC in the work of Seckler and colleagues (*14*). The protrimer therefore undergoes a conformational alteration to reach the native state, yet without a significant change in net surface charge. The similar surface charge densities represent the sum effect of all exposed amino acids of these species as they migrate through the electrophoretic field. Hence, it is likely that some of the specific residues that contribute to the net surface charge are different between protrimer and native trimer, but the net effect of these residues is the same.

What is the molecular basis for the larger radius of protrimer? Previous experiments have indicated that folding of the central β-helix domain is one of the early steps in native trimer formation (*14*). These results suggest that while the β-helix region is likely compact and docked in the protrimer intermediate, either the N-terminus or interdigitated C-terminus may be non-native. This conformational difference for the protrimer would likely lead to a larger size, slowing the progress of this species through a polyacrylamide gel. The C-terminal domain, which requires intricate interdigitation, is a likely site for a final conformational transition during the conversion from protrimer to the native state.

Single amino acid change mutants were employed to probe the conformational changes that take place during the conversion of protrimer to native trimer. Ferguson plots for the mutant proteins report on the environment of specific sites on the tailspike polypeptide chain. The effect of the G177R substitution on gel mobility was very similar for both the G177R protrimer and native trimer species. This result suggests that residue 177 is exposed both in the native trimer fold, and also the protrimer conformation. The three additional exposed positive charges of G177R presumably account for the altered mobility of the mutant species with respect to the wild-type species.

The R382S mutation results in the loss of three positive charges from each trimeric tailspike species. Nevertheless, the Ferguson plot for the R382S mutant protein native trimer was very similar to that of the wild type native trimer (Figure 7B). This probably represents the fact that the residue 382 side chain is buried in the native tailspike crystal structure and therefore makes only a minor contribution to the net surface charge (*15*). However, the free mobility (Y-intercept) of the R382S protrimer was quite different from the mobility of the wild type protrimer, indicating a less-positive net surface charge. This result suggests that the S382 side chain is exposed in the protrimer and buried in the native trimer. The protrimer therefore is not only a less compact form of native trimer, but has a unique conformation, with some different exposed residues.

The G435R mutant protein results in the addition of three positive charges to the native tailspike trimer and protrimer. The Ferguson plot for the G435R mutant native trimer is quite different than the plot of the wild type native trimer (Figure 7C). The smaller Y-intercept (Table 3) indicates that the mutant native structure has a more positive net surface charge, consistent with an interpretation that the three positive charges introduced by the G435R mutation are at least partially solvent exposed in the native trimer structure. In addition, the native trimer Ferguson plot also has a less negative slope than that of the wild-type native trimer. Ferguson plot theory interprets this result as a molecular radius for the G435R native trimer smaller than that of the wild-type trimer (Table 3) (*27*). Yet, given that the mutation introduced three bulky amino acid side chains, it is unlikely that the radius of the mutant protein significantly decreased, especially since it is known that the G435R mutation has no effect on the activity or native state stability of the mutant protein (*41*). Instead, we suspect that the arginine side chains form salt bridges with negatively charged residues elsewhere in the structure, and/or that the arginine side chains restricts a breathing or unwinding dynamic motion of the wild-type protein, thus reducing the apparent dimensions. The G435R protrimer Ferguson plot, on the other hand, is very similar to the wild-type protrimer plot, suggesting that this amino acid substitution interferes more with the native trimer structure than with the protrimer conformation.

While previous results have indicated that the β-helix region is relatively well formed in the protrimer (*14*), it is possible that residue 435 is not exposed in the intermediate because of shielding from another part of the polypeptide chain, such as the C-terminus. The transition between protrimer and native trimer may therefore involve the disassociation of the C-terminal amino acid residues from the β-helix domain, followed by interdigitation. Such an intertwining would create a more compact protein, yet because the large β-helix domain has already formed, there would not be a radical difference in the surface-exposed side chains. The more compact native trimer would thus migrate faster in a nondenaturing polyacrylamide gel, consistent with our experimental results (Figures 3 and 4). Although the results of this study indicate that the conformational differences between protrimer and native trimer are concentrated toward the C-termini of the polypeptide chains, this study is unable to distinguish between alternative conformations of the C-terminal residues. Examination of the folding behavior of other tailspike C-terminal mutations may provide a more complete description of the molecular details of the Pt → Nt conversion.

Effect of Redox Condition on the Protrimer Intermediate. The native tailspike trimer has eight reduced and buried cysteine residues (*46*). In the folding and assembly of the wild-type protein, interchain disulfide bonds are formed in the protrimer intermediate and then reduced (*25*). Thus, during refolding in vitro there is no net change in the redox state of the protein from the reduced denatured chains to the reduced native trimer. Nonetheless, it seemed likely that the tailspike folding pathway could be stalled after protrimer formation through manipulation of the refolding redox

conditions. In fact, we were unable to increase the concentration of the protrimer intermediate with altered refolding redox conditions. The protrimer band was faint—when present—in experiments with predominantly GSH, presumably because GSH increased the rate of Pt → Nt conversion. For ratios high in GSSG, the protrimer band was faint to absent. It was accompanied by a diffuse trimeric band, referred to previously as trimeric aggregate (*33*) that was not protrimer, as it migrated slightly faster. This species could represent disulfide-bonded conjugates of a trimeric intermediate with glutathione. However, protrimer and native trimer tailspike migration was unaffected by the presence or absence of glutathione in the refolding buffer. Under oxidizing conditions, neither protrimer nor native trimer accumulated, suggesting aberrant oxidation may have blocked the folding pathway at an earlier step. These results differ from those reported by Robinson and King (*25*) who found that oxidizing conditions increased the yield of native trimer using radioactively labeled tailspike protein.

In the lower temperature range of phage growth, the substitution of any one tailspike cysteine residue with serine still permits formation of correctly folded, fully functional tailspike trimers (*26*). Therefore, it may be possible for the polypeptide chains to adopt the protrimer conformation without formation of disulfide bonds, albeit at a slower rate. The temperature used in these refolding experiments (20 °C) represents the lower end of the temperature range used for tailspike folding in vivo.

Refolding Kinetics. We analyzed the refolding kinetics of these three charge-change mutations under permissive conditions (20 °C). Refolding experiments for G177R show that the refolding rate for this mutant protein was very similar to wild-type tailspike at permissive temperatures (Figure 8A). The amino acid change alters the surface charges of both protrimer and native trimer, but did not prohibit the formation of either species.

Refolding kinetic experiments demonstrate that R382S mutant tailspike also folded with an overall rate similar to that of wild type tailspike (Figure 8B). However, closer examination of the formation and disappearance of refolding intermediates shows a prolonged accumulation of monomeric intermediates, a distribution of dimeric species similar to that seen for wild type tailspike, and a reduced accumulation of the protrimer intermediate. We suspect that the change from a charged to a neutral amino acid at position 382, in addition to affecting early steps in tailspike refolding, also may have decreased the rate of conversion of monomeric and dimeric intermediates to the protrimer conformation. However, there seems to have been no negative effect on the rate of Pt → Nt conversion. This reinforces the results from the Ferguson plot analysis, which suggest that the R382S mutation had a more dramatic effect on the structure of the protrimer, rather than the native trimer.

The refolding kinetics for the G435R mutant tailspike were very different from that seen for wild type tailspike. The G435R protein folds very slowly when compared to wild-type tailspike. Ferguson plot analysis indicates that the G435R protrimer is similar in shape and net charge to the wild-type protrimer, yet production of the G435R protrimer was retarded. Presumably, while the mutation of residue 435 may not disrupt the surface charge or shape of the mutant protrimer, the mutation does alter an interaction that promotes the formation of the protrimer species. The conversion of the G435R protrimer to native trimer is also retarded. These results underscore our assignment of G435 as a site influencing the Pt → Nt conversion.

Tailspike folding intermediates represent complex structural hierarchies, not accessible through study with conventional spectroscopic methods. Studies of the conformation of ribosome-bound tailspike polypeptide chains (*19*) and early in vitro refolding intermediates (*14*, *21*) have demonstrated that organization of the β-helix domain is an early folding event. However, the formation of native structure formation during later folding and assembly steps is dependent on interactions between subunit polypeptide chains. As a result, studies of the tailspike folding pathway cannot be fully elucidated by examination of the folding of individual domains. As protein folding studies broaden to include a wider range of native state structures and sizes, it will likely be necessary to develop novel approaches to study larger, more complex folding intermediates. The gel electrophoresis analysis described here has proved very useful for studying the complex folding and assembly pathway of a large multisubunit protein.

ACKNOWLEDGMENT

We thank Anne Robinson and Robert Seckler for helpful discussions, and Stephen Raso for reading the manuscript and assistance with the kinetic simulations and global fitting algorithm. We thank Kay Finn and Jesse Boehm for assistance with refolding experiments.

REFERENCES

1. Gerstein, M. (1998) *Fold. Des. 3*, 497−512.
2. Royer, W. E., Jr., Strand, K., van Heel, M., and Hendrickson, W. A. (2000) *Proc. Natl. Acad. Sci. U.S.A. 97*, 7107−7111.
3. Engel, J., and Prockop, D. J. (1991) *Annu. Rev. Biophys. Biophys. Chem. 20*, 137−152.
4. Kreisberg, J. F., Betts, S. D., and King, J. (2000) *Protein Sci. 9*, 2338−2343.
5. van Raaij, M. J., Mitraki, A., Lavigne, G., and Cusack, S. (1999) *Nature 401*, 935−938.
6. Lehman, K., Ho, C. K., and Shuman, S. (2001) *J. Biol. Chem. 276*, 14996−15002.
7. Ban, N., Nissen, P., Hansen, J., Moore, P. B., and Steitz, T. A. (2000) *Science 289*, 905−920.
8. Buevich, A., and Baum, J. (2001) *Philos. Trans. Royal Soc. London B Biol. Sci. 356*, 159−168.
9. Milla, M. E., Brown, B. M., Waldburger, C. D., and Sauer, R. T. (1995) *Biochemistry 34*, 13914−13919.
10. Gloss, L. M., and Matthews, C. R. (1998) *Biochemistry 37*, 15990−15999.
11. Waldburger, C. D., Schildbach, J. F., and Sauer, R. T. (1995) *Nat. Struct. Biol. 2*, 122−128.
12. Sinclair, J. F., Ziegler, M. M., and Baldwin, T. O. (1994) *Nat. Struct. Biol. 1*, 320−326.
13. Smith, D. H., Berget, P. B., and King, J. (1980) *Genetics 96*, 331−352.
14. Fuchs, A., Seiderer, C., and Seckler, R. (1991) *Biochemistry 30*, 6598−6604.
15. Steinbacher, S., Miller, S., Baxa, U., Budisa, N., Weintraub, A., Seckler, R., and Huber, R. (1997) *J. Mol. Biol. 267*, 865−880.
16. Steinbacher, S., Seckler, R., Miller, S., Steipe, B., Huber, R., and Reinemer, P. (1994) *Science 265*, 383−386.
17. Clark, P. L., Liu, Z. P., Rizo, J., and Gierasch, L. M. (1997) *Nat. Struct. Biol. 4*, 883−6.
18. Parker, M. J., Dempsey, C. E., Lorch, M., and Clarke, A. R. (1997) *Biochemistry 36*, 13396−13405.

19. Clark, P. L., and King, J. (2001) *J. Biol. Chem. 276*, 25411−25420.
20. Goldenberg, D., and King, J. (1982) *Proc. Natl Acad. Sci. U.S.A. 79*, 3403−3407.
21. Danner, M., and Seckler, R. (1993) *Protein Sci. 2*, 1869−1881.
22. Betts, S. D., and King, J. (1998) *Protein Sci. 7*, 1516−1523.
23. Goldenberg, D. P., Smith, D. H., and King, J. (1983) *Proc. Natl. Acad. Sci. U.S.A. 80*, 7060−7064.
24. Danner, M., Fuchs, A., Miller, S., and Seckler, R. (1993) *Eur. J. Biochem. 215*, 653−661.
25. Robinson, A. S., and King, J. (1997) *Nat. Struct. Biol. 4*, 450−455.
26. Haase-Pettingell, C., Betts, S., Raso, S. W., Stuart, L., Robinson, A., and King, J. (2001) *Protein Sci. 10*, 397−410.
27. Hames, B. D. (1981) in *Gel Electrophoresis of Proteins: A Practical Approach* (Hames, B. D., and Rickwood, D., Eds.) pp 1−147, Oxford University Press, New York.
28. Goldenberg, D. P., and Creighton, T. E. (1984) *Biochemistry 138*, 1−18.
29. Haase-Pettingell, C., and King, J. (1997) *J. Mol. Biol. 267*, 88−102.
30. Winston, F., Botstein, D., and Miller, J. H. (1979) *J. Bacteriol. 137*, 433−439.
31. King, J., and Yu, M.-H. (1986) *Methods Enzymol. 131*, 250−266.
32. Yamamoto, K. R., Alberts, B. M., Benzinger, R., Lawhorne, L., and Treiber, G. (1970) *Virology 40*, 734−744.
33. Speed, M. A., Wang, D. I., and King, J. (1995) *Protein Sci. 4*, 900−908.
34. Sather, S. K., and King, J. (1994) *J. Biol. Chem. 269*, 25268−25276.
35. Kuzmic, P. (1996) *Anal. Biochem. 237*, 260−273.
36. Seber, G. A. F., and Wild, C. J. (1989) *Nonlinear Regression*, Wiley, New York.
37. Marquardt, D. W. (1963) *J. Soc. Ind. Appl. Math. 11*, 431−441.
38. Ferguson, K. A. (1964) *Metabolism 13*, 985−1002.
39. Tietz, D., Aldroubi, A., Schneerson, R., Unser, M., and Chrambach, A. (1991) *Electrophoresis 12*, 46−54.
40. Yu, M. H., and King, J. (1988) *J. Biol. Chem. 263*, 1424−1431.
41. Sturtevant, J. M., Yu, M. H., Haase-Pettingell, C., and King, J. (1989) *J. Biol. Chem. 264*, 10693−10698.
42. Newcomer, M. E. (1995) *FASEB J. 9*, 229−239.
43. Gronenborn, A. M., Filpula, D. R., Essig, N. Z., Achari, A., Whitlow, M., Wingfield, P. T., and Clore, G. M. (1991) *Science 253*, 657−661.
44. Kreisberg, J., Haase-Pettingell, C., and King, J. (2002) *Protein Sci. 12*, in press.
45. Fessler, J. H., and Fessler, L. I. (1978) *Annu. Rev. Biochem. 47*, 129−162.
46. Raso, S. W., Clark, P. L., Haase-Pettingell, C., King, J., and Thomas, G. J., Jr. (2001) *J. Mol. Biol. 307*, 899−911.

BI0115582